Research Article

pISSN: 2345-5357
eISSN: 2423-4214

APPLIED FOOD BIOTECHNOLOGY, 2024, 11 (1):e15
Journal homepage: www.journals.sbmu.ac.ir/afb

Design and Synthesis of a New Anticancer and Antimicrobial Nanocomposite by Microalgae Based on an Up-down Approach

Marjan Rajabi, Mahdi Rahaie*, Hossein Sabahi

Department of Life Science Engineering, Faculty of New Sciences and Technologies, University of Tehran, Tehran 14399-57131, Iran.

Abstract

Background and Objective: Use of natural ingredients is a safe efficient approach to overcome various diseases. Encapsulated ginger extract has shown improved physicochemical characterizations, compared with that, the ginger extract has. In this study, a natural system integrated with ginger bioactive compounds (6-gingerol) and green microalgae of *Chlorella vulgaris* was reported to increase bioactive compounds medicinal effectiveness and introduce a novel food supplement.

Material and Methods: First, nanoparticles of microalgae were produced using ball-milling technique. Ethanolic ginger extract, loaded on microalga nanoparticles, was investigated at various pH values (2-7.4) to effectively release the active agents. Various analytical techniques (e.g., Fourier transform infrared, thermogravimetric analyses) were used to characterize the nanocomposite and investigate its anticancer and antimicrobial effects.

Results and Conclusion: Dynamic light scattering showed a medium size of 20.9 nm for the microalga nanoparticles. The release assay of ginger polyphenols showed a releasing process controlled by the pH. Fourier transform infrared, thermogravimetric analysis and differential thermal analysis revealed adsorption of ginger extract on nano *Chlorella vulgaris* surface. Moreover, 2,2-diphenyl-picrylhydrazyl bioassay results on the nanocomposite (GE@nano C.v) verified its significant antioxidant, antibacterial and anticancer activities. The nanocomposite has the minimum inhibitory effect on human breast adenocarcinoma cells and bacterial growth at 1 and 6.25 mg ml^{-1} concentrations, respectively. In brief, adsorption of ginger extract on the microalga nanoparticle surfaces enhanced physical and chemical characteristics of the ginger extract, compared to its free form. Bioactive compounds in *Chlorella vulgaris* and ginger extract strengthen their reported activities. Furthermore, microalgal nanoparticles could act as a safe carrier for the controlled release of 6-gingerol in addition to their nutraceutical characteristics.

Conflict of interest: The authors declare no conflict of interest.

How to cite this article

Rajabi M, Rahaie M, Sabahi H. Design and Synthesis of a New Anticancer and Antimicrobial Nanocomposite by Microalgae Based on an Up-down Approach. Appl Food Biotechnol. 2024; 11 (1): e15. http://dx.doi.org/10.22037/afb.v11i1.43923

Article Information

Article history:
- Received 19 Nov 2023
- Revised 17 Jan 2024
- Accepted 17 Feb 2024

Keywords:
- Antitumor
- Food supplement
- Ginger
- Microalgae
- Natural nanomedicine

***Corresponding author:**

Mahdi Rahaie *

Department of Life Science Engineering, Faculty of New Sciences and Technologies, University of Tehran, Tehran 14399-57131, Iran.

Tel: +98-21-86093408

E-mail: mrahaie@ut.ac.ir

1. Introduction

By decreasing consumption of essential nutrition, various chronic diseases emerge. This dilemma needs a reliable effective solution to prevent future malnutrition illnesses. Nowadays, plant and algal-derived supplies as functional foods are attracting public attentions due to healthful bioactive components and their therapeutic effects [1,2]. One of the wide subgroups of algae includes microalgae. Algal biomass includes diverse health-beneficial bioactive compounds such as fibers, carotenoids, polysaccharides, polyphenols and peptides that are resulted from various metabolic pathways and effective on cardiovascular diseases (CVDs), types of cancers, atherosclerosis, neurodegenerative diseases, obesity, gut health, bone health, inflammation, type II diabetes and antioxidant and antiviral activities [3,4]. In developing seaweeds and microalgal foods, aspects such as consumer awareness and demands, bioactive compound bioavailability and stability, cost-effectiveness and life durability needs further attentions. Moreover, only a few species of microalgae are approved for the human consumption as foods due to strict food safety regulations. These include *Arthrospira platensis* (spirulina), *Chlorella* spp., *Aphanizomenon flosaquae*, *Schizochytrium* spp., *Scenedesmus* spp., *Dunaliella salina*, *Tetraselmis chuii*, *Haematococcus pluvialis* and *Porphyridium purpureum* as

resources of human nutrition within the microalgal species [5,6]. It has been reported that bioactive agents are critical for better health conditions. Therefore, plant phytochemicals have been selected as they include generally favorable characteristics such as less toxicity and well bearing by normal body cells. Frequently assessed bioactive compounds in plant extracts include curcumin, gingerol, β-carotene, quercetin and linamarin, which are developed as anticancer drugs. These compounds are rich in active agents such as phenols, alkaloids, flavonoids and tannins, which include high anti-inflammatory, antioxidant, antimicrobial, anticancer and antiaging activities [7,8].

One of the active agents of the ginger (*Zingiber officinale*) rhizome is found in the polyphenol group of 6-gingerol, which is popular for the protection of several cancers. The 6-gingerol mechanism includes interfering with a number of cell signaling pathways that affect balances between the cell proliferation and apoptosis [9]. These lead to effective approaches majorly for liver carcinoma and breast cancer. In addition, antiviral, antimicrobial, antihyperglycemic, antilipidemic, cardioprotective and immunomodulatory activities have been shown. However, 6-gingerol disadvantages such as pH and oxygen sensitivities, temperature lability, light instability and poor aqueous solubility limit its potential administrations. Thus, novel approaches for efficient delivery of 6-gingerol in a targeted controlled manner is critically important [10]. Drug delivery paths have been improved with developing of nanotechnology science. Appropriate drug-delivery nanosystems are used to enhance drug stability, specificity and durability in human blood circulatory system. Various drug vehicles have been introduced to improve drug efficiency and therapeutic effects. Some nanotechnology systems used for targeted drug delivery include dendrimers, micelles, carbon nanotubes, nanoparticles and liposomes, which are extensively used in various industries such as cosmetic, food, medicine, health, energy, electronics and environment industries [11,12]. Additionally, nanotechnology has provided a path; in which, well-qualified and practical forms of foods with nutrient bioavailability can be produced. Moreover, most of the recent studies is dedicated to crop and food processing developments through nanotechnology [13].

One of the nanotechnology approaches in food technology includes a top-down approach that uses nanostructures from bulk materials by size decreasing via milling, nanolithography or accurate-engineering techniques. In contrast to nanostructures with a large surface area-to-volume ratio, this nano-approach induces a higher activity and enhances performance. Factors such as non-specificity, low stability and aggregation can delay these nanotechnologies' uses because of decreased functions. To extend stability of nanosize structures, associating a host material (as a matrix or support) can be an alternative way to overcome the former issues [13-15]. Ginger is an old additive and traditional medicine; previous studies on using ginger extract for therapeutic approaches have been less effective, compared with the loaded ones in a carrier due to less stability and low solubility. Therapeutic characteristics of this natural medicine are limited as previously stated. Moreover, *Chlorella* (*C.) vulgaris* is approved by the Food and Drug Administration (FDA) with nutritional and medicinal characteristics and potential of uses as a natural carrier. To enhance physiochemical characteristics of ginger extract, containing health-promoting bioactive compounds, as well as natural ingredient demands in food nutraceutical and medical industries, a nanocomposite was designed that was a novel approach to overcome disadvantages of using ginger extract alone. In this study, a nano-microalga was synthetized using up-down path as a carrier for ginger extract. Moreover, composite was assessed using several bioassays.

2. Materials and Methods

2.1. Materials

Ginger rhizome was purchased from a local market in Tehran, Iran. Moreover, 2,2-diphenyl-1-picrylhydrazyl (DPPH), Folin-Ciocalteu reagent, Gallic acid and sodium carbonate were purchased from Sigma-Aldrich, USA. Methanol (purity>99%) and ethanol (purity≥99.7%) were provided by Merck, Germany. Fresh *C. vulgaris* microalgae was provided by the Faculty of New Sciences and Technologies, University of Tehran, and cultured before use. All the chemicals included analytical grades and deionized water was used to prepare solutions.

2.2. Microalgae culture

Briefly, BG-11 liquid media were used to propagate *C. vulgaris*. Microorganism was inoculated at 10% using 500-ml flasks of 200 ml of BG-11. Culture flasks were incubated using rotary incubator at 25 ℃ ±2 and 100 rpm. Cells were harvested by centrifugation (Awel, model MF 20-R, France) at 8000 rpm for 10 min at 4 ℃. These were freeze-dried (Operon, model FDB 5503, South Korea) [16].

2.3. Ginger extraction

Ginger rhizomes were dried at room temperature (RT) and grounded using blender and then the fine powder was stored at -20 ℃ for further use. Extraction method (maceration technique) reported by Ali, et al. was used with modifications [17]. Generally, 5 g of the ginger powder were transferred into a 50-ml tube and extracted with 25 ml of 70% ethanol at 26 ℃ for 72 h using shaker-incubator. The hydroalcoholic extract was filtered through Whatman filter papers (Whatman, UK) to separate from the solid phase. Concentrated extract, achieved using rotary evaporator and freeze-drier, was stored at 4 °C until use.

2.4. Characterization of the ginger extract

2.4.1. Total phenol content of the ginger extract

To investigate total phenolic content of the extract, Folin–Ciocalteu method was used [18]. Gallic acid calibration curve was plotted using mixture of ethanolic solution of Gallic acid (1 ml) and Folin–Ciocalteu reagent (200 µl, 10× diluted) and sodium carbonate (160 µl, 0.7 M). Absorbance ratio of the solution was read using UV-Vis spectrophotometer (Thermo, WPA, Germany) at 760 nm. To assess the total phenolic content, ginger extract was mixed with the highlighted reagent and the absorbance ratio was measured with three replicates. Equation 1 was used for the calculation of total phenolic compounds as follows.

$T = C \wedge V/M$ Eq. 1

Where, T was the total phenolic content [mg g^{-1} sample extract in Gallic acid equivalents; C was the concentration of Gallic acid established from the calibration curve (mg ml^{-1})]; V was volume of the extract (ml); and M was mass of the sample extract (g) [19]. Results were expressed as µg of ginger extract ml^{-1} of supernatant based on the calibration equation. Calibration equation of the ginger polyphenols (6-gingerol) was achieved via UV [absorbance value = 0.0507 (ginger polyphenols concentration in mg ml^{-1}) - 0.0636 (R^2 = 0.991)].

2.4.2. High-performance liquid chromatography analysis

Waters liquid chromatography apparatus, including a separation module (Waters 2695, USA) and a photodiode array detector (PDA) (Waters 996, USA) was used for high-performance liquid chromatography (HPLC) analysis. Data acquisition and integration were carried out using Millennium 32 software. Injection was carried out using auto-sampler injector. Chromatographic assay was carried out on a 15 cm × 4.6 mm with pre-column, Eurospher 100-5 C18 analytical column provided by Waters (sunfire) reversed-phase matrix (5 µm) (Waters, USA) and eluting was carried out in a gradient system with ACN as the organic phase (Solvent A) and distilled water (DW) (Solvent B) with a flow-rate of 1 ml min^{-1}. Injection volume was 20 µl and temperature was set at 25 °C (run time, 40 min and columns size, 2.1 mm) [20].

2.5. Size decreases in nanoscale, dynamic light scattering and zeta potential

Nano-microalgae powder with nanometer dimensions was produced using ball-milling technique (600 rpm, 6 h). Ball-milling process was carried out at 27 ℃, to avoid excessive heating. Temperature was controlled using air-cooling system. After the process, samples were transferred into a closed container to prevent moisture. The most common technology for assessing particle sizes based on particle-light interactions is dynamic light scattering (DLS) technique. Assessment of the nano C.v size was carried out using particle size analyzer (Horiba, SZ100 model, Japan). A critically physical parameter to identify surface charges of a particle (microalgae, GE, nano C.v and GE@nano C.v) in suspensions, which could anticipate interactions, is zeta potential analysis (ζ). Technically, ions around the particles dispersed in the fluid regulate charges of the particle surface layer. In this study, zeta potential was assessed using Smoluchowski formula (Eq. 2) as follows.

$$Z = \mu \frac{\eta}{\varepsilon}$$ Eq. 2

Where, η was viscosity of the media, ε was the permittivity and µ was the electrophoretic mobility [21]. In this study, zeta potential of the samples (ginger extract, micro *C. vulgaris* cell, nano *C. vulgaris*, GE@micro C.v and GE@nano C.v) homogenized in deionized water via ultrasound technique was assessed (Malvern, model ZEN 3600, UK).

2.6. Adsorption experiment

Ethanolic ginger extract was adsorbed onto *C. vulgaris* surface as a function of stirring time and ginger extract dosage. A suspension of 5 mg ml^{-1} nano C.v and 0.5 mg ml^{-1} ginger extract was stirred for 1, 2, 4, 6, 8, 10 and 12 h and then centrifuged (5000 rpm, 15 min). The harvested GE@ nano C.v (ginger extract on nanoparticles of *C. vulgaris*) was freeze-dried. As the adsorption yield curve (%) reached a plateau pattern after 1 h, this time was selected as the stirred time. Various quantities of GE (0.1, 0.2, 0.4, 0.6, 0.8 and 1 mg ml^{-1}) were suspended in flasks containing 5 mg ml^{-1} nano C.v (dissolved in 70% ethanol), stirred for 1 h and then centrifuged (5000 rpm, 15 min). The harvested GE@nano C.v was freeze-dried. Polyphenol assessment (especially 6-Gingerol) of ginger extract adsorbed onto nano C.v was carried out as follows: 1 ml of the solution was collected and centrifuged (5000 rpm, 15 min). Supernatant was separated from the sediment and re-centrifuged (12,000 rpm, 10 min). Concentration of the GE was calculated at 760 nm, using UV-visible spectroscopy (Thermo, WPA, Germany) [16]. Encapsulation efficiency (EE%) and encapsulation yield (EY%) were calculated using Eqs. 3 and 4:

$$\text{Encapsulation efficiency (\%)} = \frac{Mass\ of\ encapsulated\ GE}{Total\ initially\ added\ GE\ mass} \times 100$$ Eq. 3

$$\text{Encapsulation yield (\%)} = \frac{Mass\ of\ encapsulated\ GE}{Mass\ of\ the\ resulted\ nanocomposite} \times 100$$ Eq. 4

2.7. Verification of adsorption

To verify adsorption of ginger extract on nano Alg surface, Fourier transform-infrared spectroscopy (FTIR), thermogravimetric analysis (TGA) and differential thermogravimetric analysis (DTA) were carried out.

2.7.1. Thermogravimetric analysis

The TGA was carried out at a heating rate of 10 ℃ min^{-1} from RT to 600 ℃ with the inert nitrogen gas of 50 ml min^{-}

[1] using thermal gravimetric analyzer (TGA/DSC/1, Mettler Toledo, Singapore).

2.7.2. Differential thermogravimetric analysis

The DTA analysis of the GE, nano C.v and nano Alg/GE was carried out to assess physical state of the extract in this carrier and possibility of the interactions between the GE and the microalga.

2.7.3. Fourier transform-infrared spectroscopy

Chemical characteristics of the material were investigated using FTIR spectroscopy (Perkin-Elmer Frontier, USA) using KBr disks in the range of 400–4000 min^{-1}.

2.7.4. Antioxidant assay (total antioxidant capacity)

Photochemical stabilities of the nanocomposite (GE@ nano C.v) and ginger extract were assessed via a procedure described by Paramera et al. [22] with minor modifications. Free GE (200 mg) and a quantity of each nanocomposite (containing 200 mg of ginger polyphenols) were exposed to sunlight for a month using enclosed glass Petri dishes. Time of the light exposure included 12 h day^{-1} with a total of 720 h. The average daily temperature within the month was 25 ℃. After exposure for 7, 14 and 30 d, samples were collected and bioactivities of their 6-gingerol were assessed as follows: antioxidant activity of dispersed GE and nanocomposite (GE@nano C.v) were assessed using DPPH free radical scavenging method [23]. Inhibition of DPPH radicals by the samples was calculated using Eq. 5 as follows.

$$\text{DPPH inhibition (\%)} = \frac{A\ control - A\ sample}{A\ control} \times 100 \quad \text{Eq. 5}$$

Where, $A_{control}$ was the absorbance spectrum without GE and A_{sample} was the absorbance of ginger polyphenol nanocomposite.

2.8. *In vitro* assays

2.8.1. Antibacterial assay

Staphylococcus aureus ATCC 33591, *Pseudomonas aeruginosa* ATCC 9027, *Salmonella enterica* ATCC 9270 and *Escherichia coli* ATCC 10536 were selected for the antibacterial susceptibility assay. Minimal inhibitory concentrations (MICs) of the ginger extract and nanocomposite were assessed using microtube dilution assay as described by Acharya and European Committee for the highlighted bacterial strains. Ethanolic extract concentrations of 2.5, 1.25 and 0.625 mg ml^{-1} and nanocomposite concentrations of 1-4 mg ml^{-1} (consisting of ginger extract) were prepared using serial dilution in LB broth and 0.5 McFarland standard (10^8 CFU ml^{-1}) of the bacterial suspensions was added to each tube. All tubes were incubated at 30 °C for 14 h at 100 rpm. Absorption of each sample was measured at 600 nm using UV-vis spectroscopy (Thermo, WPA, Germany). The lowest extract concentration that inhibited bacterial growth was recorded as MIC (in three independent experiments) [24]. Inhibition of the bacterial growth was calculated using Eq. 6 as follows.

$$\text{Antibacterial activity (\%)} = \frac{A\ positive\ control - A\ sample}{A\ positive\ control} \times 100 \quad \text{Eq. 6}$$

Where, $A_{positive\ control}$ was the absorbance spectrum without samples (ginger extract and nanocomposite) and A_{sample} was the absorbance of bacteria with certain concentrations of ginger extract and nanocomposite. Culture media was used as blank.

2.8.2. Cytotoxicity assay

In this study, human breast adenocarcinoma MCF-7 cell line was cultured using T-25 cell culture flasks containing Hi-Gluta XL Dulbecco's Modified Eagle's Medium (DMEM) supplemented with 10% fetal bovine serum (FBS), streptomycin (100 µg ml^{-1}) and penicillin (100 U ml^{-1}). Cells were propagated using cell culture incubator supplied with 5% CO_2 at 37 ℃. cells were seeded overnight using 96-well cell culture plates and RPMI media suspension of three treatments (ginger extract, nano C.v and GE@nano C.v) was added to the wells at a confluence of 70% to avoid possible interferes of DMEM media with the samples (200 µl total volume). The control wells included no agents. Experiments were carried out with three replicates. Effects of each treatment on cancer cell growth were assessed after 24, 48 and 72 h, separately. After treatment of cells with various concentrations of the samples (0.5, 0.75 and 1 µg ml^{-1}) in each well for 24, 48 and 72 h, cells were rinsed with 1× PBS buffer and incubated with 100 µl of 0.5 mg ml^{-1} MTT at 37 ℃. After 4 h of incubation, 100 µl of DMSO were added to dissolve the dark-blue crystals of formazan (MTT metabolites) and incubated for 30 min at 37 ℃. Then, absorbance of the reduced MTT was measured at 560 nm using plate reader device (Convergys ELR 96×, Germany) [25].

2.9. Statistical analysis

Data represent mean ±SD (standard deviations) of three replicates. The mean comparisons were carried out using one-way variance analysis (ANOVA). Antioxidant activity data of nanocomposite and ginger extract were analyzed in a completely randomized block design with three replicates and three treatments (exposure to sunlight for 0, 14, 30 and 60 d). Duncan multiple range test (p<0.05) was used to assess significance of the difference within the treatment means. Data for each analysis were represented as the mean ±SE (standard error) of the mean.

3. Results and Discussion

3.1 High-performance liquid chromatography analysis

The HPLC analysis was carried out to quantify 6-gingerol as a bioactive compound (polyphenol) with therapeutic characteristics as well as antioxidant activities.

Chromatograms in Fig. 1b show spectra associated to ginger extract as well as the standard spectra of 6-gingerol (Fig. 1a). Peaks linked to 6-gingerol at 14.38 min were clearly present in the two spectra, showing 6-gingerol in the ginger extract. Using data, standard curve of 6-gingerol was first plotted and then quantity of 6-gingerol in the ginger extract was calculated as 96 mg g^{-1} DW (dry weight) extract (Fig. 1 c). This value was higher than that by Yamprasert et al. (2020), where concentration of 6-gingerol in the extract was calculated as 71.13 mg g^{-1} using soaking method [26]. Compared to the method by Simonati et al. (2009) that calculated 170 mg g^{-1}, the former value was lesser, which could be due to the use of supercritical fluid[1] extraction technique and high pressure for extraction in that study [27].

3.2. Release assay

Release assessment of 6-gingerol in the ginger extract was carried out based on the absorbance at 760 nm in the simulated environment of body conditions with pH 7.4 using Folin-Ciocalteu reagent at various times. Since extract was loaded on nanoparticles of the microalgae, further releases were expected at the beginning. At t = 1 h in the acidic conditions similar to the stomach with pH 2, the release rate was 16% and at pH 7.4, the rate was 14%. Up to 72 h, the release rate was constant with mild changes and reached 18% (Fig. 2). Complete release of the ginger extract was not observed at no pH conditions. However, release of the extract in acidic conditions of the stomach was higher, which was due to the effects of acidic pH on interactions between the algal nanoparticles and the extract as well as the surface load. According to Zarei et al., release rates of gingerol loaded in pegylated and non-pegylated nanoliposome respectively were 3.1 and 4.8% within 48 h [28]. Release rate in report of Jafari et al. was nearly 39% within 2 h and 59% within 4 h [16]. In another study by Shateri et al., release comparison of two synthetic systems (BCE-Spirulina and BCE-nanosized Spirulina) was investigated in physiological (pH 7.4) and acidic (pH 1.2) conditions within 96 h. Release rates of the extract were respectively calculated as 50 and 40% within the first 12 h. Based on the results, release of extract from the nanocomposite was faster and higher at the two pH conditions because of loading further extracts on the *Spirulina* surface, compared with the microalgal whole cell. The plateau curve was seen after 48 h, which reached 50% in acidic pH [29].

3.3. Dynamic light scattering and zeta potential assessments

To assess sizes of the ground *C. vulgaris* nanoparticles, an appropriate quantity of the microalgal nanoparticles was first dissolved in DW and sizes of the particles were assessed after sonication for 15 min. Sizes of *Chlorella* nanoparticles included 20.9 nm. Sharp peak and high height of the peak ndicated the high number of the particles (90%) in this size range (Fig. 3). Furthermore, *C. vulgaris* included three growth phases of log, stationary and lag phases. In the early log phase, a fragile unilamellar layer with 2-nm thickness could be demonstrated. Through maturation (log phase), cell wall thickness gradually increased to 17-20 nm, forming a microfibrillar layer of glucosamine. Due to the variation of cell wall rigidity of *C. vulgaris* within the growth phase, appropriate digestion and absorption of the valuable nutritional substances were limited [30]. Therefore, nano-sized microalgae were used not only to overcome problems of the ginger extract adsorption onto the *Chlorella* surface, but also to enhance drug loading efficiency of the synthetic nanocomposite.

Naturally, surface groups, extracellular products and cell structures affect electric characteristics of cells. In physiological pH, zeta potentials of the ginger extract (GE), *C. vulgaris* (microalgae), nanoparticles of *C. vulgaris* (nano C.v), microcomposite (GE@micro C.v) and nanocomposite (GE@nano *C.v*) included -22.8, -16.8, -27.2, -4.3 and -9.3 mV, respectively (Fig. 4). Based on the results, the lowest quantity of the extract could be loaded on the particles of *C. vulgaris*, this occurred due to the negative surface charge and repulsion in loading process. The whole cell of *C. vulgaris* included a negative surface charge of -16.8 mV; similar to that of Hao, et al., which linked to cell wall compositions of majorly cellulose, hydroxyl(-OH), carboxyl(-COOH) and aldehyde(-CHO) groups with negative charges [31]. Surface charge of the nanocomposite was -9.35 mV, becoming further positive and closer to the charge of the extract that indicating better adsorptions of the ginger extract on the microalgal nanoparticles. Zeta potential of the synthesized nanocomposite could be addressed as the reason for the low adsorption of ginger on the microalgal surfaces. Results showed that by shrinking the size of *C. vulgaris* particles from micrometers to 20 nm (less than 100 nm) with effects on physical characteristics, its surface charge became further negative and closer to -30 mV; thus, its stability increased due to the increases in the ratio of surface to volume [32]. Moreover, surface charge of the ginger extract was -22.8 mV, similar to that reported by Min Ho et al. This was because of the presence of carbohydrates and numerous anion sites, lipids and polyphenols due to possible groups in the extract [33].

3.4. Fourier transform-infrared spectroscopy analysis

Figure 5 shows FTIR graphs of ginger extract, microalgae and nanocomposite (GE@nano C.v), to indicate chemical groups in each treatment individually and characterize their interactions in synthetized nanocomposite.

[1] SC-CO2

A

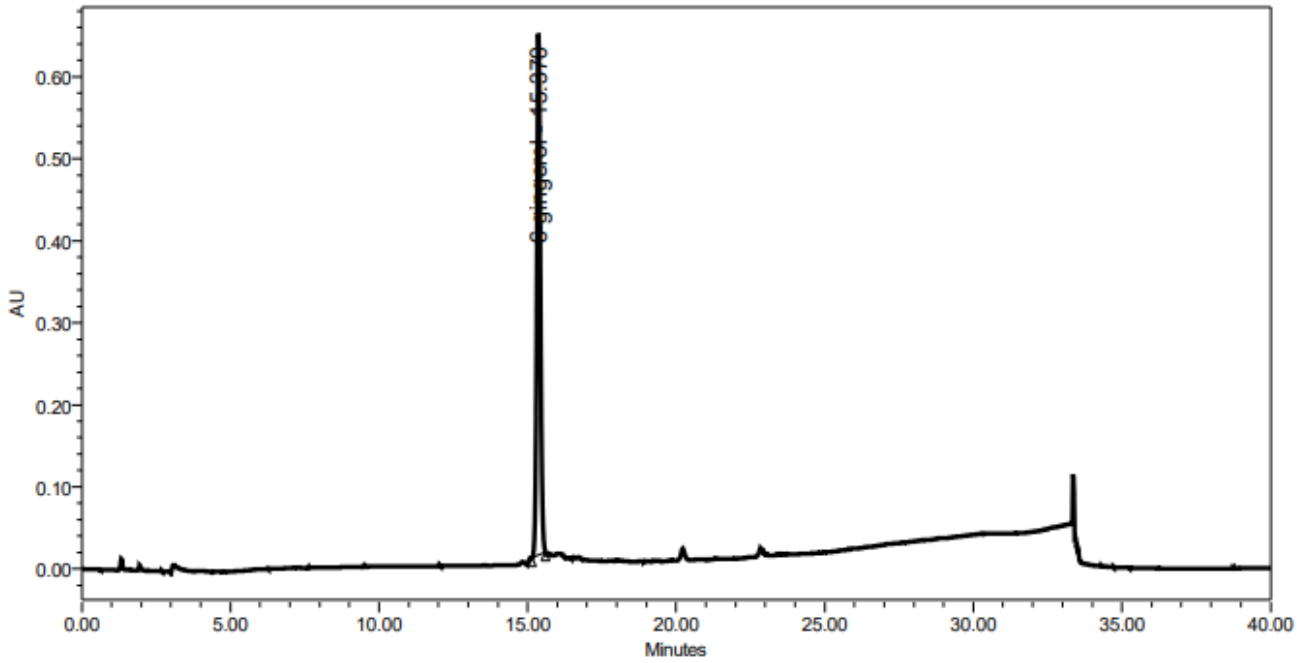

	Peak Name	RT	Area	% Area	Height
1	6-gingerol	15.370	5337667	100.00	634913

B

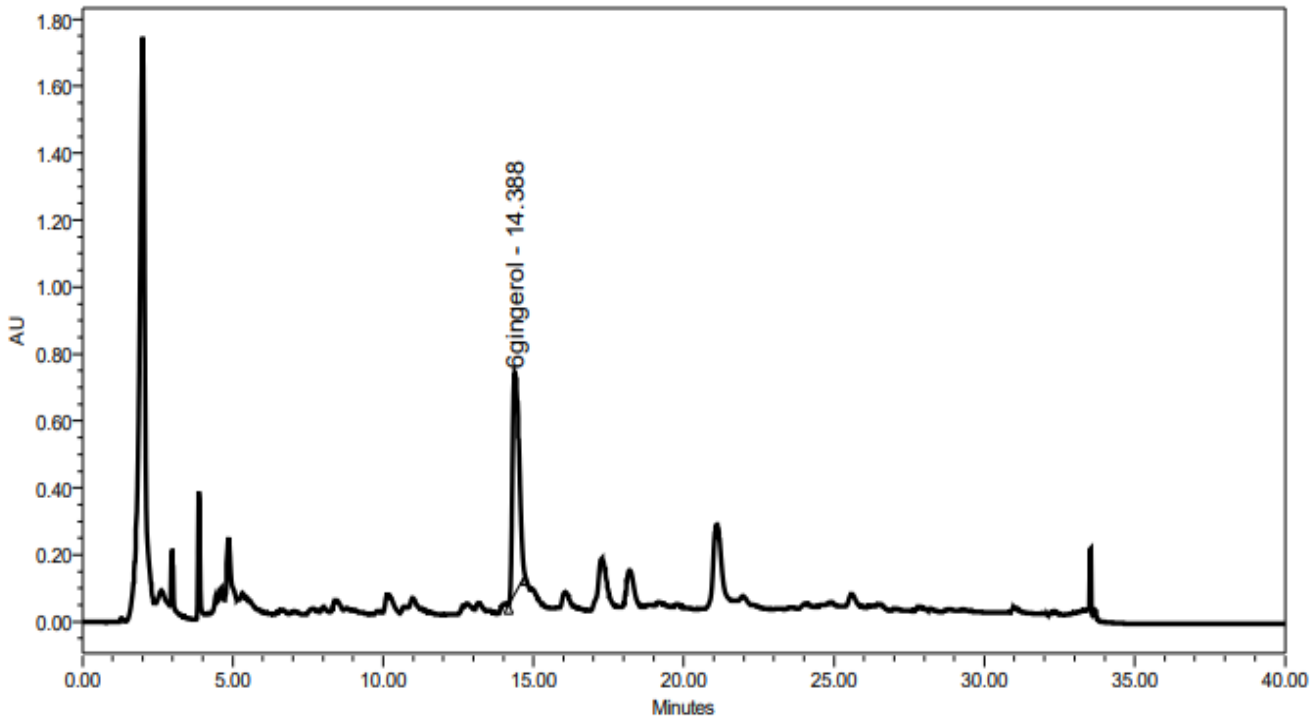

	Peak Name	RT	Area	% Area	Height
1	6gingerol	14.388	9687957	100.00	660282

C

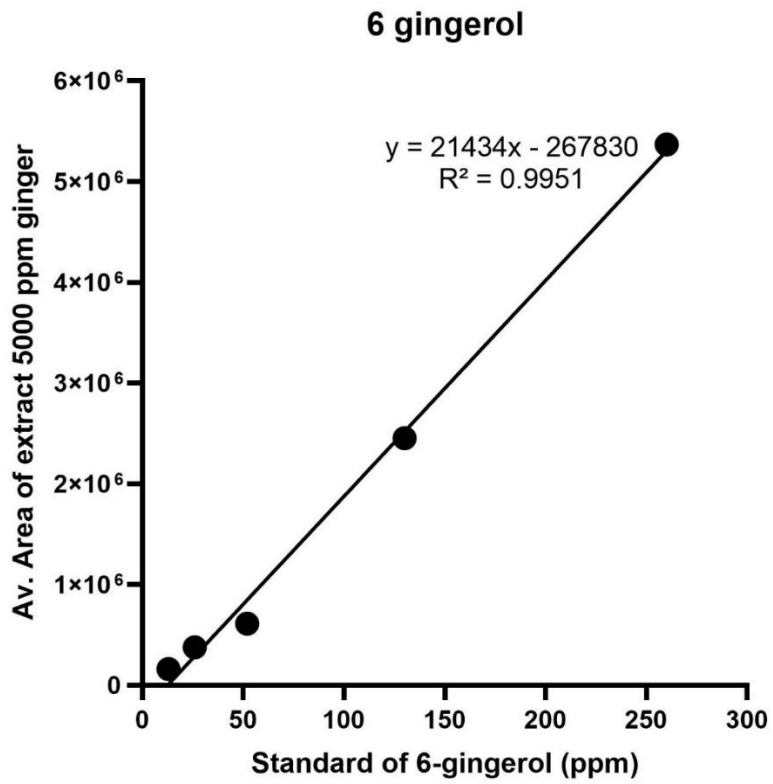

Figure 1. High-performance liquid chromatography peaks corresponding to 6-gingerol standard (260 ppm) (a), ginger extract (b) and 6-gingerol content of the ginger extract (c).

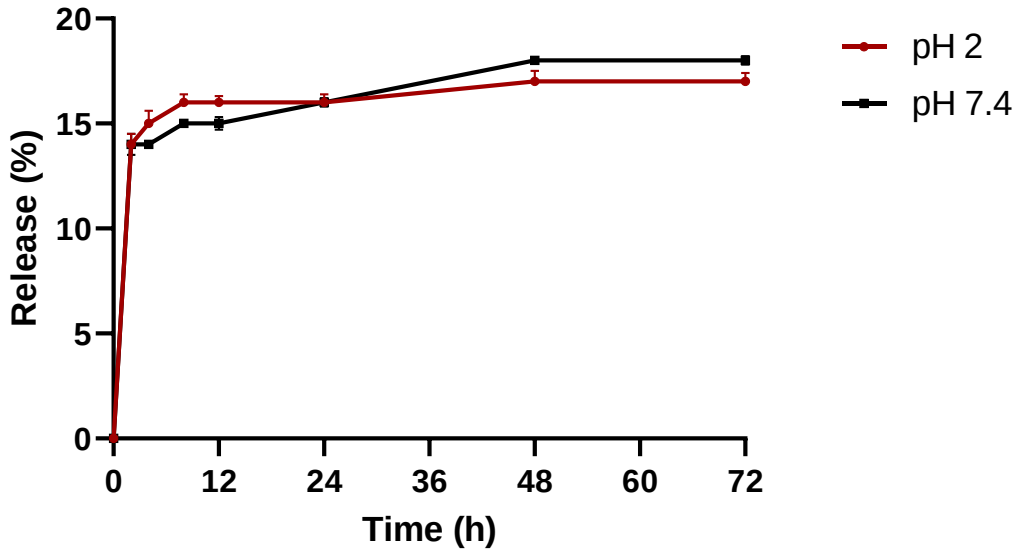

Figure 2. Release rate curves of the ginger extract from nanocomposite at two acidic (red line) and neutral (black line) pH values.

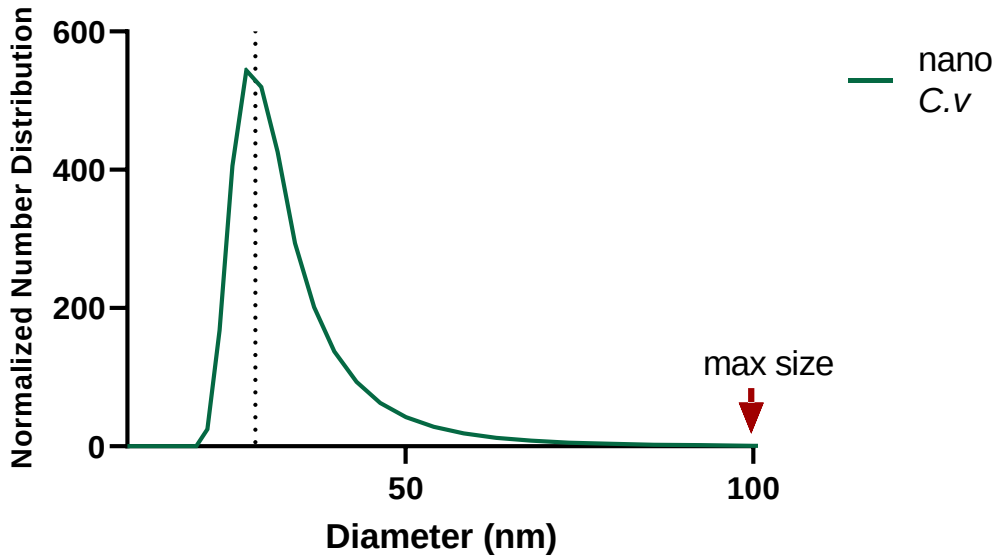

Figure 3. The size measurement of *Chlorella vulgaris* particles after milling by DLS technique. Most of the particles' sizes are in the average of 20.9 nm.

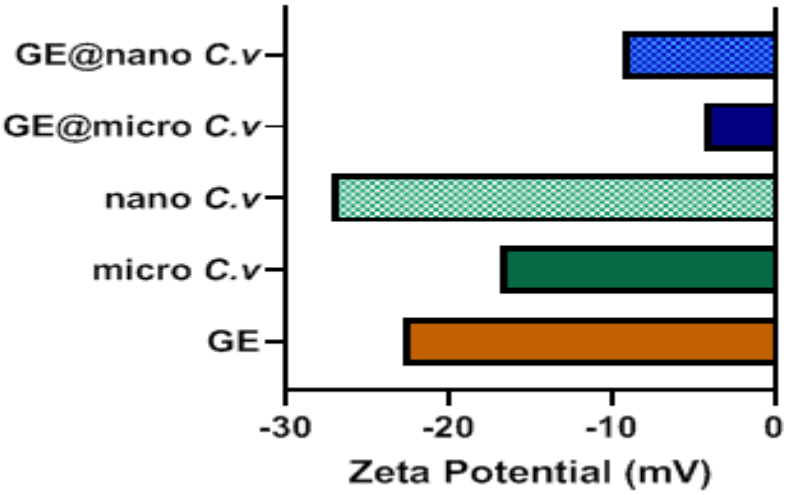

Figure 4. Surface charges (zeta potentials) of the four samples. GE (orange), *Chlorella vulgaris* whole cell (green), *Chlorella vulgaris* nanoparticles (green pattern), microcomposite (blue) and nanocomposite (light blue pattern).

3.4.1. The ginger extract

The strong band located in the area of 3527.24 $cm^{-1}$was linked to alcohol groups (O-H) and the presence of intramolecular and intermolecular hydrogen bonds; which could be associated to carbohydrates and polyphenols in the extract. The peak in the area of 2916.69 cm^{-1}showed asymmetric stretching vibration of the C-H group and possibly the carboxyl group [34]. In addition, FTIR spectrum of the ginger included a relatively strong peak at 1606.5 cm^{-1}, which was in the range of 1600–1609 $cm^{-1}$and linked to the ring of polyphenols. The absorption spectrum in 1515.8 belonged to the nitro-aromatic groups of ginger extract. The broadening of the peak in the area of 1500–1800 indicated double and amide bonds. Moreover, C=O stretching bonds and N-H bending bonds when showing a broad peak in the range of 1516-1863.86 centered on the 1638 cm^{-1} area. Presence of a 1268.13 cm^{-1}peak was associated to the vibrations of alkyl ether and ester groups, demonstrating presence of triglycerides in the extract [35]. Furthermore, peak of 1040.10 cm^{-1} included bending vibrations of the C-C bond of cellulose extract [33]. Absorption bands in the area of 924.45 cm^{-1}were linked to carbon-carbon double bonds [36].

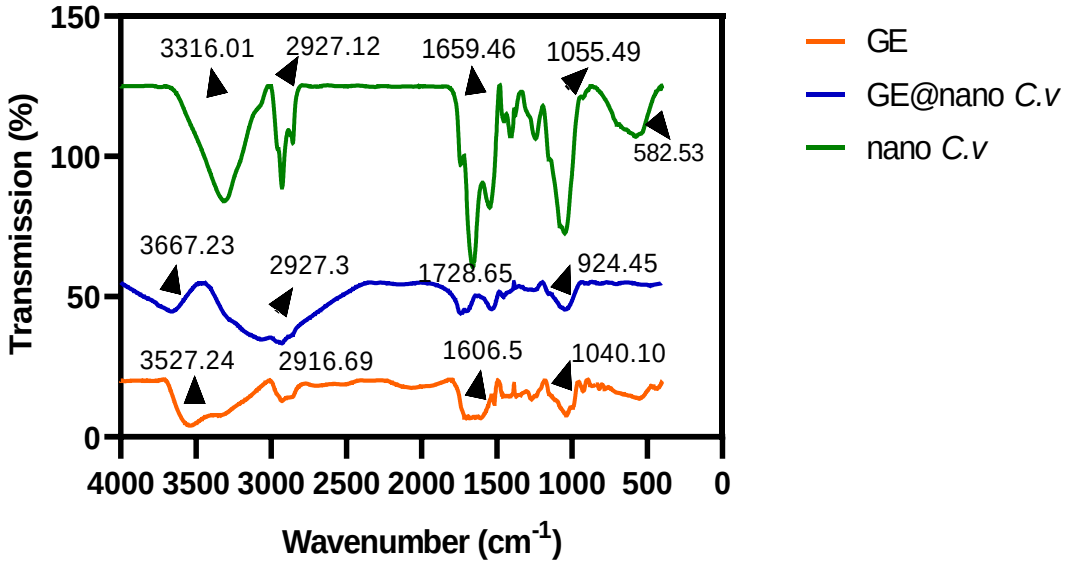

Figure 5. Fourier transform-infrared spectroscopy spectra of the ginger extract (GE, orange), nanocomposite (GE@nano C.v, blue) and nano *Chlorella vulgaris* (nano C.v, green).

3.4.2. Microalgae

Spectrum of *C. vulgaris* microalgae showed several peaks in various areas. The band of 3316.01 cm^{-1} corresponded to the O-H stretching group, revealing presence of a strong alcohol group. Area of 1659.46 cm^{-1} showed a strong band, sign of the presence of the first type of amide group within the proteins. Band of 2927.12 cm^{-1}demonstrated presence of lipids in microalgae [37]. Band in the area of 2855.44 cm^{-1}showed the bending CH_2 group linked to carbohydrates and lipids. Band in the area of 1738.96 cm^{-1} highlighted ester bond of the carbonyl group. Peak in the area of 1547.97 cm^{-1}belonged to the proteins and C=O stretching group. Presence of peaks in the areas of 1406.05 and 1242.77 $cm^{-1}$was linked to the carbon-carbon bending group and the carboxylic acid group of microalgae, respectively. Peak of 1072–1099 cm^{-1} was associated to -O-C group of carbohydrates, nucleic acids and other phosphate-containing compounds. Moreover, peak of 980–1072 cm^{-1}belonged to the group (C-O-C) of polysaccharides [16,38].

3.4.3 Nanocomposite

Nanocomposite spectrum was located between the FTIR spectra of extract and microalga with further similarity to the extract, which could be attributed to loading of the extract on the microalgae. In FTIR spectra of the nanocomposite, bands were removed, replaced or decreased in depth. Band in the range of 3500–3300 cm^{-1} of the spectra of the extract and microalga nanoparticles shifted to the left (3667.23cm^{-1}) in the spectra of the nanocomposite, revealing connections of the extract with microalga. Lack of 3527 cm^{-1}peak of the extract could be due to the interactions of O-H group of phenol with microalga. In contrast, 2927 cm^{-1}peak of *Chlorella* became wider in the present nanocomposite, which was possibly due to the interactions of microalga with the extract. The microalga peak shifted from 1738 to 1728.65 $cm^{-1}$and the extract from 1515 to 1534.94 cm^{-1}in the nanocomposite could be due to the interactions of microalgal proteins with the extract through C=O and N-H groups, respectively. Peak in 1047 cm^{-1} area of the extract could be seen in the spectra of the nanocomposite. Peaks between 924 and 564 cm^{-1} in the extract and peaks between 1242 and 582 cm^{-1} of *Chlorella* in the nanocomposite were removed, demonstrating interactions between the extract and microalga and the formation of C-C and C-O single bonds.

3.5. Thermogravimetric analysis assay

Investigating thermal stability (Fig. 6), graph of microalga showed its three-stage mass losses due to the pyrolysis process (25-600 ℃), which ultimately led to 70% decreases in the mass of microalga. Biomass's type and composition could change the TGA curve. In the first stage, mass losses occurred due to dehydration [16]. Nearly 4.65% of the microalga mass decreased as water evaporation up to 117 °C occurred (moisture loss). Small changes in the slope of the graph at 117-201 °C could be due to the beginning of the decomposition of compounds such as hemicellulose and carbohydrates. By increasing the temperature to values higher than 117 ℃, the second stage of biomass degradation began with a sharp slope (major zone).

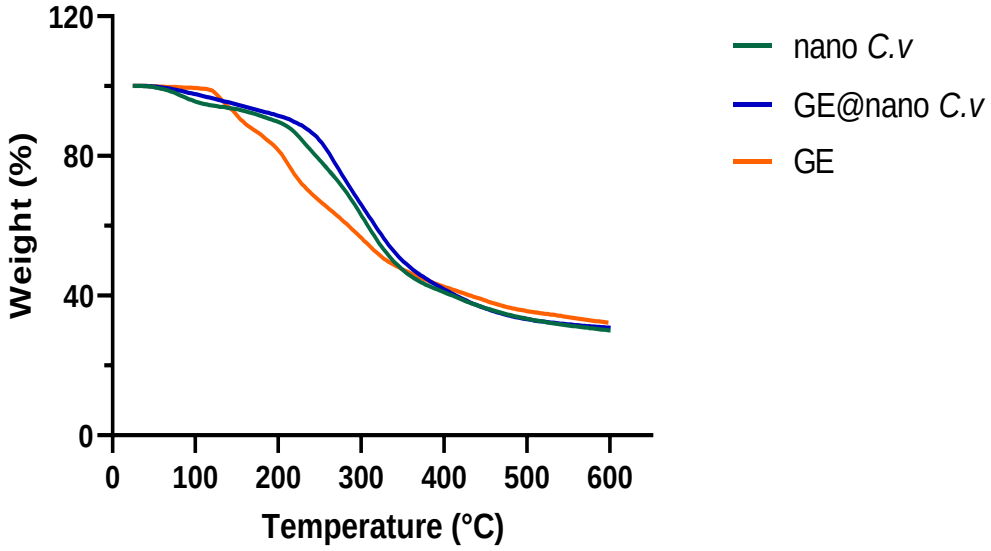

Figure 6. Thermogravimetric analysis of the three samples: nano C.v (green), nanocomposite (blue) and ginger extract (orange).

Hence in the temperature range of 201–379 °C, nano C.v biomass quickly decreased by 46%, which could be caused by decomposition of the components. Volatile compounds such as organic materials, proteins, lipids, carbohydrates and cellulose and at higher temperatures (up to 379 °C), lignin, carbon materials and minerals (nearly 12% wt), were decomposed slowly [16,39,40]. With a low slope of the graph (third stage of 400–600 ℃), all volatile components of nano C.v were removed and non-volatile components were destroyed left as amorphous carbon forms [39]. In ginger extract graph, the mass curve decreased gradually. At 100 ℃, the first peak corresponded to the water loss (6.46%) [41]. The second weight loss occurred at 142.8–172.4 ℃, which represented decomposition of several aromatic compounds [42]. In the third stage (172.4-241.6 ℃), organic compound degradation occurred in decomposition of organic materials [43]. The last and the major step of mass loss occurred at 241.6-600 ℃ (36.6%) due to organic compound oxidation, lignin and cellulose degradation and complete decomposition [43]. The second and the third stages of GE degradation occurred at 142–241 ºC, while this range for GE@nano C.v was 210-300 ºC, meaning that synthesize of nanocomposite (GE@nano C.v) led to thermal stability of the ginger extract up to 300 ℃. In contrast, onset of the destruction temperature of microalgae was at 200 ℃. In nanocomposite graph, degradation temperature began at 150 ℃, showing that when the extract was loaded on *C. vulgaris*, degradation began earlier. As previously reported by Shetta et al. [44], green tea extract on the surface of chitosan nanoparticles was destroyed faster. This higher thermal stability of GE after adsorption on nano C.v is similar to that of Jafari et al. study, which demonstrated that thermal stability of curcumin was improved after its encapsulation into *C. vulgaris* [16]. Therefore, thermal degradation of organic compounds (the major step) in the nanocomposite occurred at higher temperatures, compared to those in ginger extract and nanomicroalga (two degradation steps). This could address improved intramolecular interactions between the ginger extract chemical groups and nanomicroalga that suggested a natural nanocomposite with enhanced thermal characteristics.

To calculate the quantity of ginger extract adsorbed on *C. vulgaris* surface, Eq. 7 by Shateri et al. [29] was used as follows.

Calculated mass residue =

$$degraded\ extract\ (\%) * x - degraded\ alage\ (\%) * (100 - x) / 100 \quad \text{Eq. 7}$$

Where, x was the load quantity (%). Based on the formula, quantity of the extract loaded on the microalga was 31.64%. Table 2 shows weight decompositions (%) of the three samples.

3.6. Differential thermal analysis

The DTA curve shows thermal difference analysis. The technique calculated differences between the sample temperature and the reference temperature. The DTA graph shows a better temperature difference, compared with the TGA curves [49]. As shown in Fig. 7, DTA curves showed degradation peaks of nano CV, GE and GE@nano CV composite. In nano C.v, a calorific peak was seen at 100 °C, revealing dehydration and water loss. A strong second peak and a weak peak at 200 °C specify thermal decomposition of various *Chlorella* compounds and beginning of their degradation.

Table 1. Comparison of the current study with similar studies using various drug carriers and their effects.

Carrier	Cargo	Loading (%)	Positive effects	Reference
Spirulina platensis	Doxorubicin	85	+ Anticancer efficacy on lung metastasis Biodegradable Improved fluorescence imaging	[45]
Spirulina platensis	Black cumin	81.94	+ Antibacterial activities + Antioxidant activities + Anticancer activities + Thermal stability	[29]
Chlorella vulgaris	Curcumin	55	+ Thermal stability + Photostability	[16]
Chlorella pyrenoidosa cells	Lycopene	96.31	+ Stability + Antioxidant activity	[46]
Polymeric micelles (TPGS/PEG-PCL)	6- Gingerol	79.68	+ Solubility of 6-gingerol + Oral bioavailability + Improved brain distribution	[47]
Nanostructured lipid carriers	6- Gingerol	76.71	Higher drug concentrations in serum + Solubility of 6-gingerol + Oral bioavailability	[48]
Chlorella vulgaris	Ginger extract	31.64	+ Antibacterial effect + Antioxidant activities + Anticancer activities + Thermal stability	This work

Table 2. Thermogravimetric analysis assay with weight decreases as the temperature changes for the three samples (nanocomposite, nano C.v and GE).

Samples	Temperature range (°C)	Weight loss (%)
Nanocomposite	25.00-157.88	5.77
	157.88-600.70	63.43
Nano *Chlorella vulgaris*	24.50-117.31	5.46
	117.31-201.39	4.90
	201.39-379.55	46.65
	379.55-600.77	12.94
Ginger extract	24.60-142.8	6.46
	142.8-172.4	6.39
	172.4-241.62	18.26
	241.62-600	36.69

The fourth strong heating peak was observed at 300 °C, which included almost destruction of the microalga [39]. In DTA curve of GE, three strong peaks were seen in the temperature range of 100-200 °C (respectively from left to right: endothermic, endothermic and exothermic); which belonged to dehydration, destruction and decomposition of the major compounds in the ginger extract. Other exothermic and endothermic peaks were seen in the range of 200-300 °C. Residual and volatile compounds and carbohydrate depolymerization of the extract were almost completely decomposed, based on the studies by Kuk et al. [50].

Diagrams of DTA of GE@nano C.v were similar to diagrams of nano C.v, showing low loads of the extract. The two peaks of nano C.v degradation at 200 and 300 °C decreased to one peak at 250 °C. This major change in the decomposition peak of nano C.v showed that GE absorption on microalga nanoparticles was so strong that caused major changes in the rate and point of its decomposition. Diagram of the nanocomposite is plotted to the left, compared to that of the extract. Interactions between the extract and the microalga decreased thermal resistance in the range of 200-300 °C, which could be caused by weak interactions. In contrast, heat flow of the microalgae and its mild changes could be due to the low superficial loading of the extract on surface of the microalga as well as weak connections caused by it. It could be interpreted at a heating rate of 10 min/°C in the first stage of the heating process with a peak at 55 °C with a molecular weight (MW) of 0.09 and a second peak of heat removal at 114 °C with an MW of 0.05 possibly due to the water loss. Thermal decomposition in the second stage was exothermic with two weak peaks at 236 °C and a strong peak at 297 °C with MWs of 0.2 and 0.35. This is the maximum heat loss due to protein decomposition at the top of the peak and carbohydrates, where bonds included O-O, N-O, C-N, C-C, C-O, N-H, C-H, N=N, H=H, O-H, O=O, C=C, C=N and C=O.

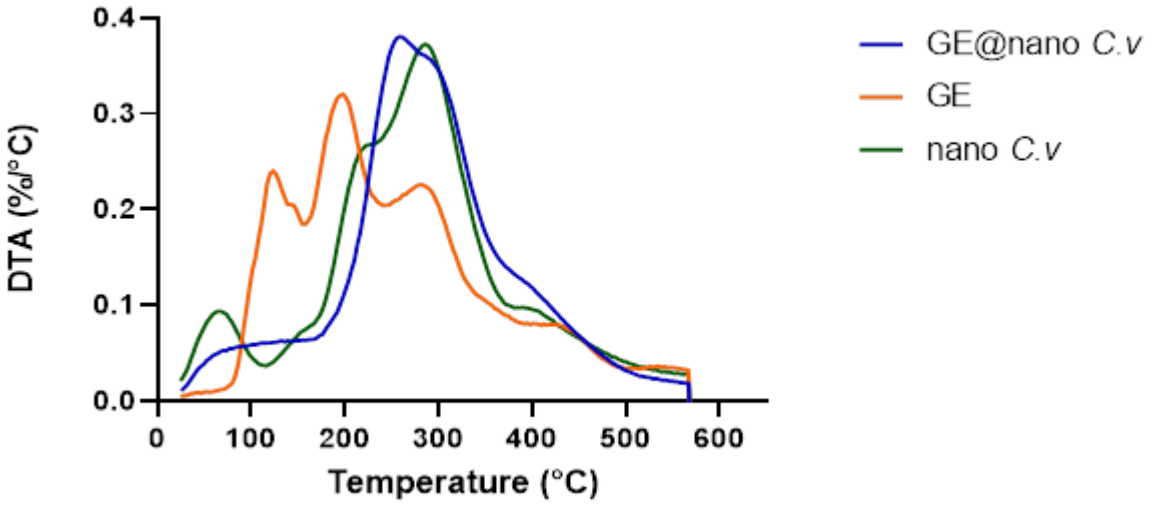

Figure 7. Differential thermogravimetric analysis diagram of nano C.v, ginger extract and nanocomposite.

Following the thermal decomposition curve, gasification occurred in the third stage with a weak peak at 370 °C and MW of 0.1. These results were similar to the results of Wang et al. [40]. In the third stage, only non-condensable gases such as CO, CO_2, H_2 and CH_4 were released with a little weight loss. This might reflect that the necessary heat was directly proportional to the increased temperature, as almost all the volatiles in the microalga were released in the thermal decomposition zone. This could be understood due to the soft structure of microalga with a relatively low lignin concentration (7.33-9.55% wt), thus volatile substances were easily separated from the tissues. Compared to hardwoods with high lignin contents (25%) and complex textures, thermal decomposition of hardwoods over 600 °C still produced non-condensable gases, explaining its relatively high weight losses.

3.7. The 2,2-diphenyl-1-picrylhydrazyl test

Ginger increases blood plasma antioxidant capacity and decreases lipid peroxidation and renal nephropathy in rats. Gunathilake et al. detected that 6-gingerol in ginger extract removed peroxide radicals and hence could be used as a natural food additive and a substitute for artificial antioxidants [51]. Antioxidant activities of the ginger extract and nanocomposite (GE@nano C.v, loaded with 0.5 mg mg ml^{-1} GE) were investigated for one month. As shown in Fig.8, antioxidant activity of the nanocomposite on the first day was nearly 60% at a concentration of 1.5 mg ml^{-1}. This increased by ~2% within one month as a result of antioxidant characteristics of *Chlorella*, when GE adsorbed on the surface within the first week and then made the antioxidant agents of *C. vulgaris* available. Karaman et al. detected that the higher activity of inhibiting free radicals for the sample encapsulated in yeast cells was associate to the higher anti-radical contents of the yeast cells [52].

In a study by Ghasemzadeh et al., antioxidant activity of the methanol extract of ginger was reported as 51-58% at a concentration of 40 µg ml^{-1} [53], possibly due to differences in the extraction method and various bioactive contents. In a study of Stoyanova et al., antioxidant activity of the ginger extract at 20 µg ml^{-1} was calculated as 90% [54]. In the study of Abdel Karim et al., *C. vulgaris* showed a 50% antioxidant activity with a concentration of 1.95 mg ml^{-1} due to the presence of plant chemicals (e.g., phenols, flavonoids, etc.) [55].

3.8. Antibacterial assay

Antibiotics are the compounds, which are used for human, animal and aquaculture treatments. Recently, their residues and degraded products in environment have included potential risks and toxicity worldwide. Antimicrobial activity against pathogenic and food-spoiling microorganisms is due to the bioactive compounds. Phenolic compounds such as gingerol and shogaol and their relationships majorly with other compounds such as β-sesquiphalendrene, cis-caryophyllene, zingiberene and α-farnesin are responsible for their antimicrobial activities in ginger essential oil and extract [56]. Hydrophobic residues of the ginger extract may interact with the lipophilic part of the cell membrane, disrupting their membrane integrity and function (e.g., electron transfer, nutrient absorption, protein and nucleic acid synthesis and enzymatic activity). In this study, results of the MIC assay showed that the ginger extract (Fig. 9a) and nanocomposite (Fig. 9b) included antibacterial charact-ristics and rates of their inhibition depended on their doses. By decreasing concentrations of the extract and nanocomposite, their antibacterial activities decreases. Concentrations of 1, 2 and 4 mg ml^{-1} of the extract and 6.25, 12.5 and 25 mg ml^{-1} of the nanocomposite were investigated.

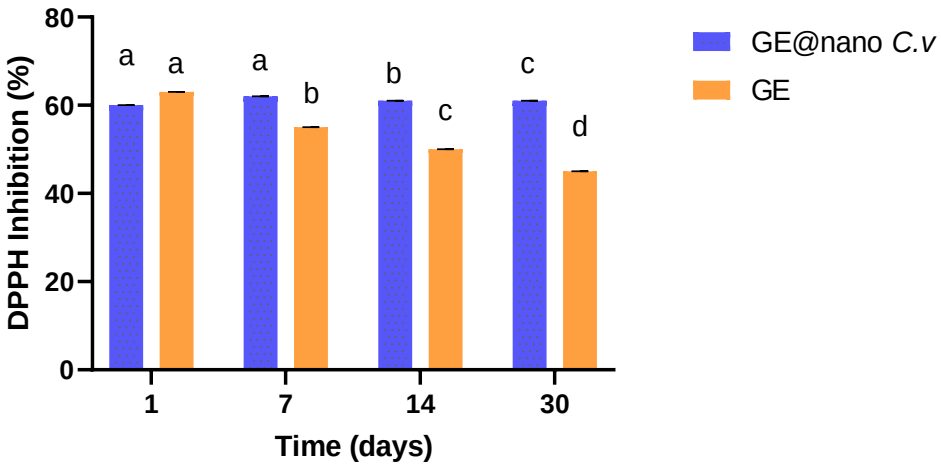

Figure 8. Antioxidant diagrams of the ginger extract (GE) and nanocomposite at concentrations of 0.5 and 1.5 mg ml^{-1}, respectively. All data are expressed as the mean ±SEM. Statistical analysis was carried out using ANOVA (letters, $p < 0.05$). Charts with similar letters include no significant differences.

Results of the antibacterial assay showed that absorption of the extract on the nanoparticle significantly decreased its antibiotic characteristics, which could be linked to the slow releases of the extract active compounds from the surface of the nanoparticles; however, this could be active for a longer time. Antibacterial activity of the ginger extract was due to its polyphenol compounds, especially zingibrene, gingerol and terpenoids [57]. Based on the study of Hussein et al., *E. coli* and *S. aureus* were susceptible to the active compounds of *C. vulgaris* at a high concentration of 100 mg ml^{-1}. This could be due to the fatty acid contents, bioactive compounds, effects on cell cycle and protein and DNA syntheses or hydrophobic interactions that ultimately lead to cell leakage and death [58]. Inhibitory effects of the ginger extract on *S. aureus*, *Pseudomonas* spp. and *E. coli* was estimated as 90%. Inhibitory effects of nanocomposite on *Salmonella* spp. was higher than 60% and its effects on *Pseudomonas* spp. reached the maximum, increasing by ~6% for *S. aureus* to 50%. These differences could occur due to the structural differences in these bacteria [59].

3.9. Cytotoxicity assay

Ginger compounds (6-gingerol and its derivatives) have been shown to decrease hazards of several diseases, majorly in the gastrointestinal tract (GIT) and cancers such as carcinogenesis in the skin and breasts [60]. To assess cell viability of the breast cancer cell line (MCF-7) for their ability to decrease tetrazolium salt [3-(4,5-dimethylthiazol-2-yl)-2,5 diphenyl tetrazolium bromide], various concentrations of GE, nano C.v and GE@nano C.v within 24, 48 and 72 h were investigated (graphs of 24 and 48-h assays not shown). Results showed outstanding cancerous-cell inhibitions by the nanocomposite (GE@nano C.v), compared to ginger extract and nano C.v. Based on the growth inhibition chart of the MTT assay in Fig. 10,

growth inhibitions of 67, 73 and 86%, were respectively reported after 24 h of incubation (37 ℃, 98% humidity, 5% CO_2), with ginger extract at concentrations of 0.5, 0.75 and 1 mg ml^{-1},. After 48 h, this value reached 28, 46 and 84%, respectively, which indicated dose and time-dependent cytotoxicity of the three treatments, as the more concentration, the higher growth inhibition. Cell viabilities were inhibited by the ginger extract treatment during 48 h. After 72 h of adding GE, cytotoxicity effects on the breast cancer cells for the concentrations of 0.5, 0.75 and 1 mg ml^{-1} were 47, 48 and 47%, respectively. It was demonstrated that anticancer activity of the ginger extract decreased within 72 *h. Various* studies have shown effectiveness of the ginger extract on tumors. However, the extract not only includes therapeutic characteristics (due to 6, 8 and 10-gingerol and 6, 8 and 10-shogaol agents) but also decreases vomiting and nausea of the patients after chemotherapy [61]. In a study by Mohammed et al., further gingerol concentrations caused higher effects on cancer cell growth inhibition as 0.1 mg ml^{-1} gingerol included significant cytotoxicity for 24 h and 0.4 mg ml^{-1} gingerol showed 80% inhibition on MCF-7 cell line [62].

As previously stated, microalgae include bioactive compounds such as phytochemicals and carotenoids (lutein in *C. vulgaris*) with verified anticancer activities [63,64]. Cytotoxicity rates included 82, 75 and 76% after 24 h of treatment with nano C.v at concentrations of 0.5, 0.75 and 1 mg ml^{-1} that reached to 96, 77 and 67% after 48 h, respectively.

A

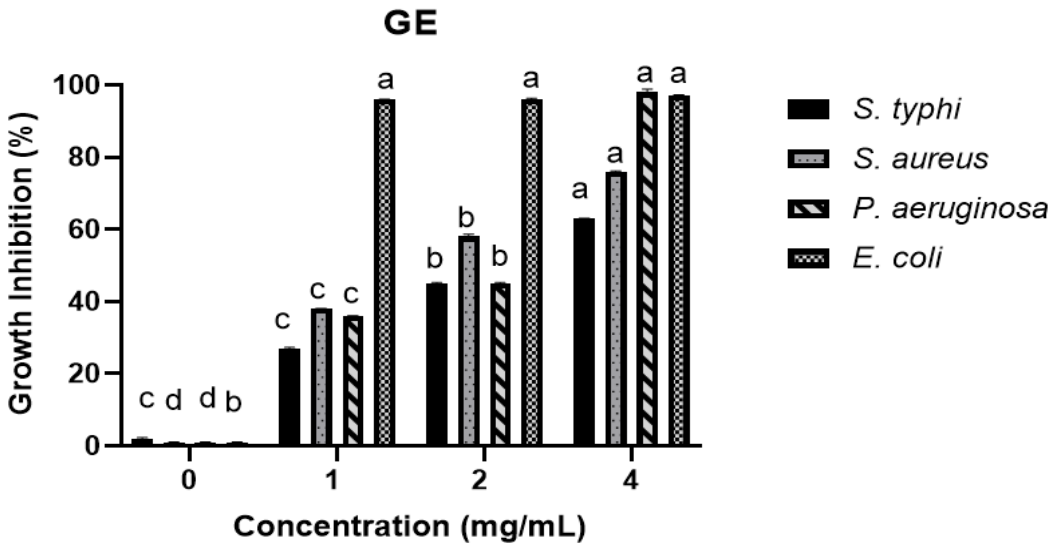

B

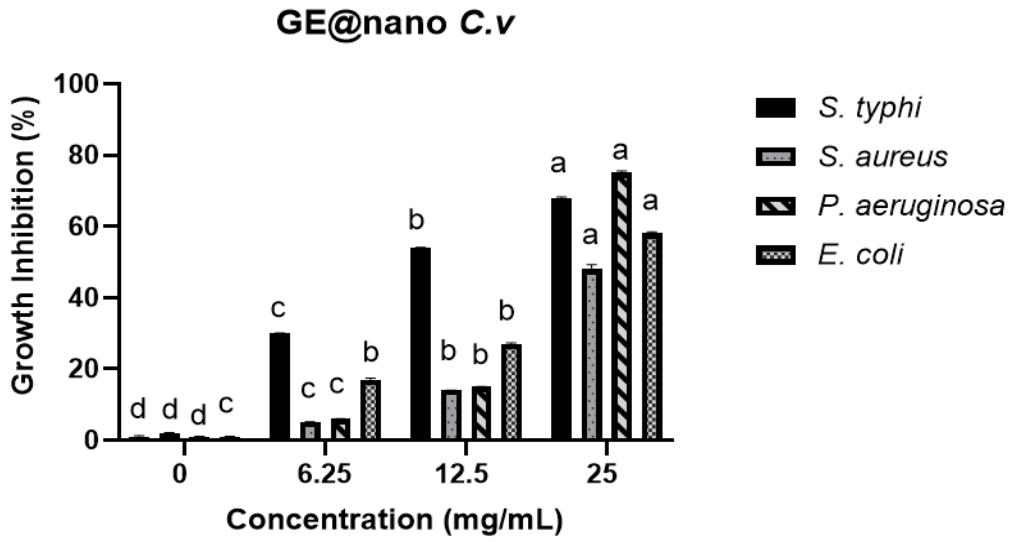

Figure 9. Graphs of the average inhibitory proportions of the ginger extract (GE) (a) and nanocomposite (b) on four bacterial strains of *Salmonella typhi* (black), *Staphylococcus aureus* (gray dotted black pattern), *Pseudomonas aeruginosa* (light gray-black pattern) and *Escherichia coli* (gray-black pattern) using MIC assay in three various concentrations with controls. Significant differences (mean ±SE) of the effects of concentrations on the bacteria is illustrated with letters at p <0.05.

Growth rates of the cancer cells at 0.5, 0.75 and 1 mg ml^{-1} respectively included 62, 62 and 67% after 72 h. This showed mild increases at 72 h, which could be due to the limited anticancer compounds in the cell wall of *C. vulgaris* microalga after grinding. Anticancer activities of the nanocomposite included 63, 63 and 71% after 24 h at 0.5, 0.75 and 1 mg ml^{-1}, respectively. After 48 h from the addition of nanocomposite, these values included 74, 71 and 59% for the concentrations of 0.5, 0.75 and 1 mg ml^{-1} with significant changes, compared to those after 24 h, respectively. After 72 h at the concentrations of 0.5, 0.75 and 1 mg ml^{-1}, growth rates of the cancer cells included 51, 54 and 53%, respectively. The maximum inhibitory effect could be seen at 1 mg ml^{-1} concentration of the nanocomposite due to the increases of ginger extract concentration adsorbed on nano *C. vulgaris*.

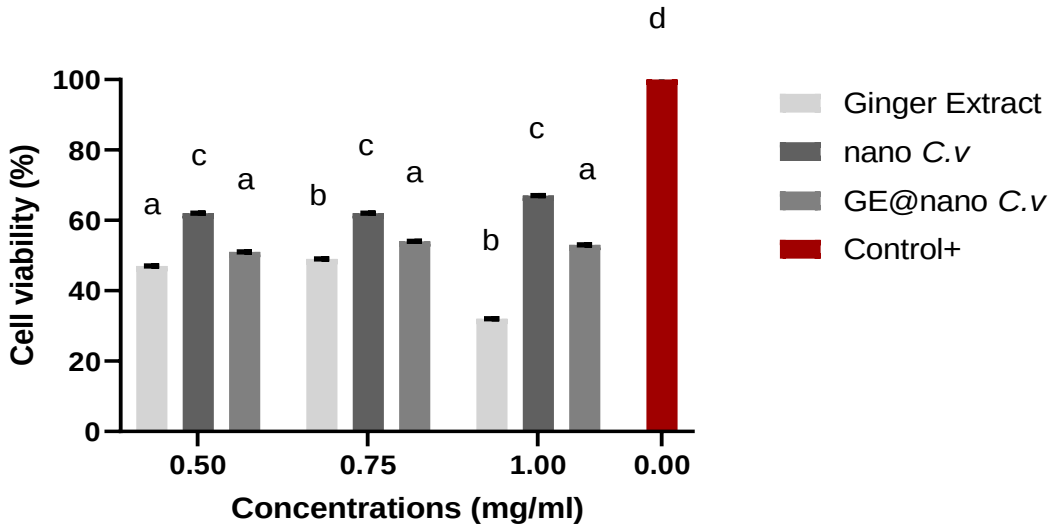

Figure 10. Cell viabilities of the cancer cells (MCF-7 cells) after incubation in 0.5, 0.75 and 1 mg ml^{-1} ginger extract, nanoparticles of *Chlorella vulgaris* and nanocomposite (GE@nano C.v) with different significant values at $p<0.05$.

Anticancer activity of the ginger extract alone decreased after 72 h. However, activity of the nanocomposite increased and was set constantly, demonstrating preservation of the activity of ginger extract adsorbed on the surface of microalga. This is a significant advantage for the use of nano C.v as a carrier for GE.

4. Conclusion

In this study, the synthesized nanocomposite included promising characteristics, which could be used in medicinal and nutritional industries. The HPLC assay showed bioactive compounds, especially 6-gingerol, in the extract (0.48 mg in 5 mg total extract). Furthermore, FTIR, TGA and DTA results verified adsorption of ginger extract on nano *Chlorella* surface. Due to intramolecular interactions of ginger with *Chlorella* chemical groups, improved thermal stability in range of 200-300 ℃ was observed. In addition, nanocomposite included a mild improved antioxidative activity within a month with 1.5 mg ml^{-1} concentration. Antimicrobial and anticancer assays indicated good effects on microbial and breast-carcinoma cell-line (MCF-7) growth at concentrations of 6.25 and 1 mg ml^{-1}, respectively. In conclusion, combination of ginger and *C. vulgaris* could improve further antioxidant, antimicrobial and antitumor effects of ginger extract, compared to ginger extract alone. Further studies are needed to focus on novel methods for increasing adsorption of ginger extract on *C. vulgaris* cell wall to enhance nanocomposite stability.

5. Acknowledgements

The authors acknowledge Prof. Ali Reza Zomorodipour from NIGEB, Iran, for his support to provide research instruments of cell culture. In addition, authors acknowledge the instrumental supports of the University of Tehran.

6. Conflict of Interest

The authors declare no conflict of interest.

References

1. Maziani S, Fadaie V, Khosravi-Darani K. Impact of spirulina platensis on physiochemical and viability of *lactobacilus acidophilus* of probiotic uf feta cheese. J Food Process Preservation . 2016; 40: 6. https://doi.org/10.1111/jfpp.12717
2. García JL, de Vicente M, Galán B. Microalgae, old sustainable food and fashion nutraceuticals. Microb Biotechnol. 2017; 10: 1017-1024. https://doi.org/10.1111/1751-7915.12800
3. Martínez-Ruiz M, Martínez-González CA, Kim DH, Santiesteban-Romero B, Reyes-Pardo H, Melendez-Sanchez ER, Ramírez-Gamboa D, Díaz-Zamorano AL, Sosa-Hernández JE, Coronado-Apodaca KG. Microalgae bioactive compounds to topical applications products- A review. Molecules 2022; 27: 3512. https://doi.org/10.3390/molecules27113512
4. Nova P, Martins AP, Teixeira C, Abreu H, Silva JG, Silva AM, Freitas AC, Gomes AM. Foods with microalgae and seaweeds fostering consumers health: a review on scientific and market innovations. J Appl Phycol 2020; 32:1789-802. https://doi.org/10.1007/s10811-020-02129-w
5. Santin A, Balzano S, Russo MT, Palma Esposito F, Ferrante MI, Blasio M, Cavalletti E, Sardo A. Microalgae-based PUFAs for food and feed: Current applications, future possibilities and constraints. J Mar Sci Eng. 2022; 10: 844. https://doi.org/10.3390/jmse10070844
6. Jacob-Lopes E, Maroneze MM, Deprá MC, Sartori RB, Dias RR, Zepka LQ. Bioactive food compounds from microalgae: An innovative framework on industrial biorefineries. Curr Opin Food Sci. 2019; 25: 1-7.

https://doi.org/10.1016/j.cofs.2018.12.003

7. Manatunga DC, de Silva RM, de Silva KMN, Wijeratne DT, Malavige GN, Williams G. Fabrication of 6-gingerol, doxorubicin and alginate hydroxyapatite into a biocompatible formulation: enhanced antiproliferative effect on breast and liver cancer cells. Chem Cent J. 2018; 12: 1-13. https://doi.org/10.1186/s13065-018-0482-6

8. Mao QQ, Xu XY, Cao SY, Gan RY, Corke H, Beta T, Li HB. Bioactive compounds and bioactivities of ginger (*Zingiber officinale* Roscoe). Foods 2019; 8: 185. https://doi.org/10.3390/foods8060185

9. Yücel Ç, Karatoprak GŞ, Açıkara OB, Akkol EK, Barak TH, Sobarzo-Sánchez E, Aschner M, Shirooie S. Immunomodulatory and anti-inflammatory therapeutic potential of gingerols and their nanoformulations. Front Pharmacol. 2022; 13: 902551. https://doi.org/10.3389/fphar.2022.902551

10. He L, Qin Z, Li M, Chen Z, Zeng C, Yao Z, Yu Y, Dai Y, Yao X. Metabolic profiles of ginger, a functional food and its representative pungent compounds in rats by ultraperformance liquid chromatography coupled with quadrupole time-of-flight tandem mass spectrometry. J Agric Food Chem. 2018; 66: 9010-9033. https://doi.org/10.1021/acs.jafc.8b03600

11. Mitchell MJ, Billingsley MM, Haley RM, Wechsler ME, Peppas NA, Langer R. Engineering precision nanoparticles for drug delivery. Nat Rev Drug Discov. 2021;20:101-24. https://doi.org/10.1038/s41573-020-0090-8

12. Singh AP, Biswas A, Shukla A, Maiti P. Targeted therapy in chronic diseases using nanomaterial-based drug delivery vehicles. Signal Transduct Target Ther 2019;4:33. https://doi.org/10.1038/s41392-019-0068-3

13. Neme K, Nafady A, Uddin S, Tola YB. Application of nanotechnology in agriculture, postharvest loss reduction and food processing: Food security implication and challenges. Heliyon 2021; 7: e08539. https://doi.org/10.1016/j.heliyon.2021.e08539

14. Guerra FD, Attia MF, Whitehead DC, Alexis F. Nanotechnology for environmental remediation: Materials and applications. Molecules 2018; 23: 1760. https://doi.org/10.3390/molecules23071760

15. Rashidi L, Khosravi-Darani K. The applications of nanotechnology in food industry. Crit Rev Food Sci Nutr. 2011; 51: 723-730. https://doi.org/10.1080/10408391003785417

16. Jafari Y, Sabahi H, Rahaie M. Stability and loading properties of curcumin encapsulated in *Chlorella vulgaris*. Food Chem. 2016; 211: 700-706. https://doi.org/10.1016/j.foodchem.2016.05.115

17. Ali AMA, El-Nour MEM, Yagi SM. Total phenolic and flavonoid contents and antioxidant activity of ginger (*Zingiber officinale* Rosc.) rhizome, callus and callus treated with some elicitors. J Genet Eng Biotechnol. 2018; 16: 677-682. https://doi.org/10.1016/j.jgeb.2018.03.003

18 Safdar MN, Kausar T, Nadeem M. Comparison of ultrasound and maceration techniques for the extraction of polyphenols from the mango peel. J Food Process Preserv. 2017; 41: e13028. https://doi.org/10.1111/jfpp.13028

19. Ganji S, Sayyed-Alangi SZ. Encapsulation of ginger ethanolic extract in nanoliposome and evaluation of its antioxidant activity on sunflower oil. Chem Pap. 2017; 71: 1781-1789. https://doi.org/10.1007/s11696-017-0164-1

20. Saldanha T, Sawaya ACHF, Eberlin MN, Bragagnolo N. HPLC separation and determination of 12 cholesterol oxidation products in fish: Comparative study of RI, UV and APCI-MS detectors. J Agric Food Chem. 2006; 54: 4107-4113. https://doi.org/10.1021/jf0532009

21. Matho C, Schwarzenberger K, Eckert K, Keshavarzi B, Walther T, Steingroewer J, Krujatz F. Bio-compatible flotation of *Chlorella vulgaris*: Study of zeta potential and flotation efficiency. Algal Res. 2019; 44: 101705. https://doi.org/10.1016/j.algal.2019.101705

22. Paramera EI, Konteles SJ, Karathanos VT. Stability and release properties of curcumin encapsulated in *Saccharomyces cerevisiae*, β-cyclodextrin and modified starch. Food Chem. 2011; 125: 913-922. https://doi.org/10.1016/j.foodchem.2010.09.071

23. Brand-Williams W, Cuvelier ME, Berset C. Use of a free radical method to evaluate antioxidant activity. LWT-Food Sci Technol. 1995; 28: 25-30. https://doi.org/10.1016/S0023-6438(95)80008-5

24. Hasan S, Danishuddin M, Khan AU. Inhibitory effect of *Zingiber officinale* towards *Streptococcus mutans* virulence and caries development: in vitro and *in vivo* studies. BMC Microbiol. 2015; 15: 1-14. https://doi.org/10.1186/s12866-014-0320-5

25. Vemuri SK, Banala RR, Subbaiah GP V, Srivastava SK, Reddy AVG, Malarvili T. Anti-cancer potential of a mix of natural extracts of turmeric, ginger and garlic: A cell-based study. Egypt J Basic Appl Sci. 2017; 4: 332-344. https://doi.org/10.1016/j.ejbas.2017.07.005

26. Yamprasert R, Chanvimalueng W, Mukkasombut N, Itharat A. Ginger extract versus Loratadine in the treatment of allergic rhinitis: A randomized controlled trial. BMC Complement Med Ther. 2020; 20: 1-11. https://doi.org/10.1186/s12906-020-2875-z

27. Şimonați CN. [6]-gingerol content and bioactive properties of ginger (*Zingiber officinale*) extracts from supercritical CO_2 extraction. Documentar study. Analele Universitatcedilla ii din Craiova-Biologie, Horticultura, Tehnologia Prelucrarii Produselor Agricole, Ingineria Mediului. 2009; 14: 609-615.

28. Zarei M, Yaraghtala S. Preparation and assessment of gingerol-loaded nanoliposomes and their effect on breast cancer cell lines (MCF-7). In Proceedings of the 4th International Conference on Researches in Science & Engineering & International Congress on Civil, Architecture and Urbanism in Asia, Bangkok, Thailand. 2019; 18.

29. Shateri F, Rahaie M, Jalili H. Chemical, functional and therapeutic properties of encapsulated black cumin extract in *Spirulina platensis*. J Food Process Preserv. 2022; 46(11): e16956.

30. Ahmad MT, Shariff M, Md. Yusoff F, Goh YM, Banerjee S. Applications of microalga *Chlorella vulgaris* in aquaculture. Rev Aquac. 2020; 12: 328-346. https://doi.org/10.1111/raq.12320

31. Hao W, Yanpeng L, Zhou S, Xiangying R, Wenjun Z, Jun L. Surface characteristics of microalgae and their effects on harvesting performance by air flotation. Int J Agric Biol Eng. 2017; 10: 125-133.

32. Sanjay SS, Pandey AC. A brief manifestation of nanotechnology. EMR/ESR/EPR Spectrosc. Charact. Nanomater, Springer; 2017. pp: 47-63. https://doi.org/10.1007/978-81-322-3655-9_2

33. Kim HJ, Lee SB, Choi AJ, Oh JM. *Zingiber officinale* extract

(ZOE) incorporated with layered double hydroxide hybrid through reconstruction to preserve antioxidant activity of ZOE against ultrasound and microwave irradiation. Nanomaterials. 2019; 9: 1281. https://doi.org/10.3390/nano9091281

34. Farmoudeh A, Shokoohi A, Ebrahimnejad P. Preparation and evaluation of the antibacterial effect of chitosan nanoparticles containing ginger extract tailored by central composite design. Adv Pharm Bull. 2021; 11: 643. https://doi.org/10.34172/apb.2021.073

35. Mehata MS. Green route synthesis of silver nanoparticles using plants/ginger extracts with enhanced surface plasmon resonance and degradation of textile dye. Mater Sci Eng. B 2021; 273: 115418. https://doi.org/10.1016/j.mseb.2021.115418

36. Zhao X, Zhu H, Chen J, Ao Q. FTIR, XRD and SEM analysis of ginger powders with different size. J Food Process Preserv. 2015; 39: 2017–26. https://doi.org/10.1111/jfpp.12442

37. Vidyadharani G, Dhandapani R. Fourier transform infrared (FTIR) spectroscopy for the analysis of lipid from *Chlorella vulgaris*. Elixir Appl Biol. 2013; 61: 16753-16756.

38. Ponnuswamy I, Madhavan S, Shabudeen S. Isolation and characterization of green microalgae for carbon sequestration, waste water treatment and bio-fuel production. Int J BioSci Biotech. 2013; 5: 17-26.

39. Agrawal A, Chakraborty S. A kinetic study of pyrolysis and combustion of microalgae *Chlorella vulgaris* using thermo-gravimetric analysis. Bioresour Technol. 2013; 128: 72-80. https://doi.org/10.1016/j.biortech.2012.10.043

40. Wang X, Hu M, Hu W, Chen Z, Liu S, Hu Z, Xiao B. Thermogravimetric kinetic study of agricultural residue biomass pyrolysis based on combined kinetics. Bioresour Technol. 2016; 219: 510-520. https://doi.org/10.1016/j.biortech.2016.07.136

41. Norhidayah A, Noriham A, Rusop M. Physical and thermal properties of Zingiber Officinale Rosc.(ginger) rhizome fine particle as a function of grinding system. Adv Mater Res. 2014, 832, 527-532. https://doi.org/10.4028/www.scientific.net/AMR.832.527

42. Hu J, Zhang Y, Xiao Z, Wang X. Preparation and properties of cinnamon-thyme-ginger composite essential oil nanocapsules. Ind Crops Prod. 2018; 122: 85-92. https://doi.org/10.1016/j.indcrop.2018.05.058

43. de Sa SC, de Souza MM, Peres RS, Zmozinski A V, Braga RM, de Araujo Melo DM, Ferreira CA. Environmentally friendly intumescent coatings formulated with vegetable compounds. Prog Org Coatings. 2017; 113: 47-59. https://doi.org/10.1016/j.porgcoat.2017.08.007

44. Shetta A, Kegere J, Mamdouh W. Comparative study of encapsulated peppermint and green tea essential oils in chitosan nanoparticles: Encapsulation, thermal stability, in-vitro release, antioxidant and antibacterial activities. Int J Biol Macromol. 2019; 126: 731-742. https://doi.org/10.1016/j.ijbiomac.2018.12.161

45. Zhong D, Zhang D, Xie T, Zhou M. Biodegradable microalgae-based carriers for targeted delivery and imaging-guided therapy toward lung metastasis of breast cancer. Small 2020; 16: 2000819. https://doi.org/10.1002/smll.202000819

46. Pu C, Tang W. Encapsulation of lycopene in *Chlorella pyrenoidosa*: Loading properties and stability improvement. Food Chem. 2017; 235: 283-289. https://doi.org/10.1016/j.foodchem.2017.05.069

47. Zhen L, Wei Q, Wang Q, Zhang H, Adu-Frimpong M, Kesse Firempong C, Xu X, Yu J. Preparation and in vitro/in vivo evaluation of 6-Gingerol TPGS/PEG-PCL polymeric micelles. Pharm Dev Technol. 2020; 25: 1-8. https://doi.org/10.1080/10837450.2018.1558239

48. Wei Q, Yang Q, Wang Q, Sun C, Zhu Y, Niu Y, Yu J, Xu X. Formulation, characterization and pharmacokinetic studies of 6-gingerol-loaded nanostructured lipid carriers. AAPS Pharmscitech 2018; 19: 3661-3669. https://doi.org/10.1208/s12249-018-1165-2

49. Jamilatun S, Budiman A. Thermal decomposition and kinetic studies of pyrolysis of *Spirulina platensis* residue. Int J Renew Energy Dev 2017; 6. https://doi.org/10.14710/ijred.6.3.193-201

50. Kuk RS, Waiga LH, Oliveira CS, Bet CD, Lacerda LG, Schnitzler E. Thermal, structural and pasting properties of brazilian ginger (*Zingiber officinale* Roscoe) starch. Ukr Food J. 2017: 674-685. https://doi.org/10.24263/2304-974X-2017-6-4-8

51. Gunathilake K, Rupasinghe HPV. Recent perspectives on the medicinal potential of ginger. Bot Targets Ther. 2015; 5: 55-63. https://doi.org/10.2147/BTAT.S68099

52. Karaman K. Characterization of *Saccharomyces cerevisiae* based microcarriers for encapsulation of black cumin seed oil: Stability of thymoquinone and bioactive properties. Food Chem. 2020; 313: 126-129. https://doi.org/10.1016/j.foodchem.2019.126129

53. Ghasemzadeh A, Jaafar HZE, Rahmat A. Antioxidant activities, total phenolics and flavonoids content in two varieties of Malaysia young ginger (*Zingiber officinale* Roscoe). Molecules 2010; 15: 4324-4333. https://doi.org/10.3390/molecules15064324

54. Stoilova I, Krastanov A, Stoyanova A, Denev P, Gargova S. Antioxidant activity of a ginger extract (*Zingiber officinale*). Food Chem. 2007; 102: 764-770. https://doi.org/10.1016/j.foodchem.2006.06.023

55. Abdel-Karim OH, Gheda SF, Ismail GA, Abo-Shady AM. Phytochemical screening and antioxidant activity of *Chlorella vulgaris*. Delta J Sci. 2020; 41: 81-91. https://doi.org/10.21608/djs.2020.139231

56. Beristain-Bauza SDC, Hernández-Carranza P, Cid-Pérez TS, Ávila-Sosa R, Ruiz-Lopez II, Ochoa-Velasco CE. Antimicrobial activity of ginger (*Zingiber officinale*) and its application in food products. Food Rev Int. 2019; 35: 407-426. https://doi.org/10.1080/87559129.2019.1573829

57. Malu SP, Obochi GO, Tawo EN, Nyong BE. Antibacterial activity and medicinal properties of ginger (*Zingiber officinale*). Glob J Pure Appl Sci. 2009;15: 3-4. https://doi.org/10.4314/gjpas.v15i3-4.48561

58. Hussein HJ, Naji SS, Al-Khafaji NMS. Antibacterial properties of the *Chlorella vulgaris* isolated from polluted water in Iraq. J Pharm Sci Res. 2018; 10: 2457-2460.

59. Acurio LP, Salazar DM, Valencia AF, Robalino DR, Barona AC, Alvarez FC, Rodriguez CA. Antimicrobial potential of *Chlorella algae* isolated from stacked waters of the Andean Region of Ecuador. IOP Conf. Ser. Earth Environ. Sci., vol. 151, Iop Publishing; 2018, p. 12040. https://doi.org/10.1088/1755-1315/151/1/012040

60. Karpagapandi L, Sultana BF. Phytochemical profiling and antioxidant activity of *Zingiber officinale* rhizome. The Pharma Innovation Journal. 2021; 10(7): 40-6.

61. Kim SD, Kwag EB, Yang MX, Yoo HS. Efficacy and safety of ginger on the side effects of chemotherapy in breast cancer patients: systematic review and meta-analysis. Int J Mol Sci. 2022; 23: 11267. https://doi.org/10.3390/ijms231911267

62. Mohammed MS. The molecular activity of gingerol on inhibits proliferation of breast cancer cell line (MCF7) through caspase activity. Ann Rom Soc Cell Biol. 2021: 11095-11103.

63. Kubatka P, Kapinova A, Kruzliak P, Kello M, Výbohova D, Kajo K, Novak M, Chripkova M, Adamkov M, Pec M, Mojzis J. Antineoplastic effects of *Chlorella pyrenoidosa* in the breast cancer model. Nutrition 2015; 31: 560-569. https://doi.org/10.1016/j.nut.2014.08.010

64. Cha KH, Koo SY, Lee D-U. Antiproliferative effects of carotenoids extracted from *Chlorella ellipsoidea* and *Chlorella vulgaris* on human colon cancer cells. J Agric Food Chem. 2008; 56: 10521-10526. https://doi.org/10.1021/jf802111x

Research Article
pISSN: 2345-5357
eISSN: 2423-4214
OPEN ACCESS

APPLIED FOOD BIOTECHNOLOGY, 2024, 11(1):e15
Journal homepage: www.journals.sbmu.ac.ir/afb

طراحی و ساخت یک نانوکامپوزیت جدید ضد سرطان و ضد میکروب با استفاده از ریزجلبک و مبتنی بر یک رویکرد بالا به پایین

مرجان رجبی، مهدی رهایی*، حسین صباحی

گروه مهندسی علوم زیستی، دانشکده علوم و فناوری های نوین، دانشگاه تهران، تهران، ایران

تاریخچه مقاله

دریافت ۱۹ نوامبر ۲۰۲۳
داوری ۱۷ ژانویه ۲۰۲۴
پذیرش ۱۷ فوریه ۲۰۲۴

واژگان کلیدی

- ضدتومور
- مکمل غذایی
- زنجبیل
- ریزجلبک
- نانو داروی طبیعی

***نویسنده مسئول**

مهدی رهایی

گروه مهندسی علوم زیستی، دانشکده علوم و فناوری های نوین، دانشگاه تهران، تهران، ایران

تلفن: ۸۱۱۱۱۸۵۸۳-۶۲+

پست الکترونیک:

mrahaie@ut.ac.ir

چکیده

سابقه و هدف: استفاده از مواد طبیعی روش کارآمد و ایمنی برای غلبه بر بیماری‌های گوناگون است. نشان داده شده است که ویژگی‌های فیزیکوشیمیایی عصاره زنجبیل ریزپوشانی شده در مقایسه با عصاره آزاد، بهبود یافته است. این مطالعه، یک سامانه طبیعی حاوی ترکیبات زیست فعال زنجبیل (۶ -جینجرول) و ریزجلبک سبز *کلرلا ولگاریس*، ترکیبات زیست فعال با اثربخشی دارویی بیشتر و مکمل غذایی جدید را معرفی می‌کند.

مواد و روش ها: ابتدا، نانوذرات ریزجلبک با روش آسیاب گلوله‌ای یا گوی‌آس[۲] تولید شدند. عصاره اتانولی زنجبیل، بارگذاری شده بر روی نانوذرات ریز جلبک، در pH های گوناگون (۲-۷/۴) مورد بررسی قرار گرفت تا عوامل فعال رهایش موثری داشته باشند. روش‌های تحلیلی گوناگونی (به‌عنوان مثال، تبدیل فوریه مادون قرمز[۳]، تجزیه و تحلیل گرما وزن‌سنجی[۴]) برای توصیف نانوکامپوزیت و بررسی اثرات ضد سرطانی و ضد میکروبی آن استفاده شد.

یافته‌ها و نتیجه‌گیری: اندازه نانوذرات ریزجلبک با روش پراکندگی نور دینامیک به‌طور متوسط ۲۰/۹ نانومتر تعیین شد. بررسی رهایش پلی‌فنول‌های زنجبیل نشان داد pH فرآیند رهایش را کنترل می‌کند. تبدیل فوریه مادون قرمز، تجزیه و تحلیل گرما وزن‌سنجی و آنالیز حرارتی افتراقی[۵]، جذب عصاره زنجبیل بر سطح نانو *کلرلا ولگاریس* نشان داد. علاوه بر این، نتایج تعیین مقدار زیستی[۶] ۲،۲-دی فنیل-پیکریل هیدرازیل بر روی نانوکامپوزیت (GE@nano C.v) فعالیت‌های قابل‌توجه ضداکسایشی، ضد باکتریایی و ضد سرطانی آن را تأیید کرد. این نانوکامپوزیت به‌ترتیب در غلظت‌های ۱ و ۶/۲۵ میلی‌گرم بر میلی‌لیتر، کمترین اثر بازدارندگی را بر روی سلول‌های آدنوکارسینومای پستان انسان و رشد باکتری‌ها دارد. به‌طور خلاصه، جذب عصاره زنجبیل بر سطوح نانوذرات ریز جلبک، ویژگی‌های فیزیکی و شیمیایی عصاره زنجبیل را در مقایسه با فرم آزاد آن افزایش داد. ترکیبات زیست فعال موجود در *کلرلا ولگاریس* و عصاره زنجبیل فعالیت‌های آنها را تقویت می‌کند. علاوه بر این، نانوذرات ریزجلبک می‌توانند علاوه بر ویژگی‌های تغذیه‌ای، به عنوان یک حامل امن برای رهایش کنترل‌شده ۶-جینجرول عمل کنند.

تعارض منافع: نویسندگان اعلام می‌کنند که هیچ نوع تعارض منافعی مرتبط با انتشار این مقاله ندارند.

[۲] Ball-milling آسیابی که در آن از گلوله‌های فولادی یا سرامیکی برای خرد و نرم کردن مواد غیرفلزی استفاده کنند

[۳] Fourier transform infrared (FT IR)

[۴] Thermogravimetric روشی تحلیلی بر مبنای اندازه‌گیری تغییرات وزن ترکیب یا آمیزه با افزایش دما

[۵] Differential thermal analysis

[۶] Bioassay تعیین قدرت یا غلظت یک مادۀ دارویی ازطریق سنجش اثرات آن بر بافت‌های زنده